

- METZ-BOUTIGUE, M.-H., JOLLES, J., MAZURIER, J., SCHOENTGEN, D., LEGRAND, D., SPIK, G., MONTREUIL, J. & JOLLES, P. (1984). *Eur. J. Biochem.* **145**, 659–676.
- MORIHARA, K. & TSUZUKI, H. (1969). *Arch. Biochem. Biophys.* **129**, 620–634.
- MOSS, D. S. (1985). *Acta Cryst.* **A41**, 470–475.
- MOSS, D. S. & MORPHEW, A. J. (1982). *Comput. Chem.* **6**, 1–3.
- MUNSHI, S. K. & MURPHY, M. R. N. (1986). *J. Appl. Cryst.* **19**, 61–61.
- NYBORG, J. & WONACOTT, A. J. (1977). *The Rotation Method in Crystallography*, edited by U. W. ARNDT & A. J. WONACOTT, pp. 139–152. Amsterdam: North-Holland.
- READ, R. J. (1986). *Acta Cryst.* **A42**, 140–149.
- ROSE, T. M., PLOWMAN, G. D., TEPLow, D. B., DREYER, W. J., HELLSTROM, K. E. & BROWN, J. P. (1986). *Proc. Natl Acad. Sci. USA*, **83**, 1261–1265.
- SARRA, R. & LINDLEY, P. F. (1986). *J. Mol. Biol.* **188**, 727–728.
- SCHADE, A. L., REINHART, R. W. & LEVY, H. (1949). *Arch. Biochem. Biophys.* **20**, 170–172.
- TAYLOR, W. R., THORNTON, J. M. & TURNELL, W. G. (1983). *J. Mol. Graphics*, **1**, 5–8.
- TEN EYCK, L. F. (1973). *Acta Cryst.* **A29**, 183–191.
- TICKLE, I. J. (1985). *Molecular Replacement*, edited by P. A. MACHIN, pp. 22–26. Daresbury: Science and Engineering Research Council.
- WEISS, W. I. & BRÜNGER, A. T. (1989). *Molecular Simulation and Protein Crystallography*, edited by J. GOODFELLOW, K. HENRICK & R. HUBBARD, pp. 16–28. Daresbury: Science and Engineering Research Council.
- WHITE, H. E., DRIESSEN, H. P. C., SLINGSBY, C., MOSS, D. S., TURNELL, W. G. & LINDLEY, P. F. (1988). *Acta Cryst.* **B44**, 172–178.

Acta Cryst. (1990). **B46**, 771–780

Complexation with Diol Host Compounds. 5. Structures and Thermal Analyses of Inclusion Compounds of *trans*-9,10-Dihydroxy-9,10-diphenyl-9,10-dihydroanthracene with 2-Butanone, 4-Vinylpyridine, 4-Methylpyridine and 2-Methylpyridine

BY DIANNE R. BOND, MINO R. CAIRA, GRANT A. HARVEY AND LUIGI R. NASSIMBENI

Department of Chemistry, University of Cape Town, Rondebosch 7700, South Africa

AND FUMIO TODA

Department of Industrial Chemistry, Faculty of Engineering, Ehime University, Matsuyama 790, Japan

(Received 23 April 1990; accepted 13 June 1990)

Abstract

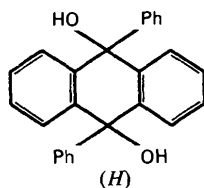
The structures of four inclusion compounds of *trans*-9,10-dihydroxy-9,10-diphenyl-9,10-dihydroanthracene with 2-butanone (1), 4-vinylpyridine (2), 4-methylpyridine (3) and 2-methylpyridine (4) have been determined by single-crystal X-ray diffraction and their thermal decomposition investigated by X-ray powder diffractometry, thermogravimetry and differential scanning calorimetry. Crystal data are: (1), C₂₆H₂₀O₂·C₄H₈O, *M_r* = 436.55, triclinic, *P* $\bar{1}$, *a* = 7.924 (1), *b* = 8.827 (2), *c* = 9.050 (1) Å, α = 109.93 (2), β = 97.31 (1), γ = 97.65 (1)°, *V* = 579.5 (2) Å³, *Z* = 1, *D_m* = 1.248 (4), *D_x* = 1.251 Mg m⁻³, Mo *K*α, λ = 0.7107 Å, μ = 0.074 mm⁻¹, *F*(000) = 232, *T* = 294 K, final *R* = 0.059 (*wR* = 0.077) for 1690 independent reflections; (2), C₂₆H₂₀O₂·2C₇H₇N, *M_r* = 574.72, monoclinic, *P*2₁/*c*, *a* = 10.045 (2), *b* = 18.630 (3), *c* = 8.419 (4) Å, β = 96.29 (3)°, *V* = 1566.0 (9) Å³, *Z* = 2, *D_m* = 1.208 (3), *D_x* = 1.219 Mg m⁻³, Mo *K*α, λ = 0.7107 Å, μ = 0.070 mm⁻¹, *F*(000) = 608, *T* = 294 K, final *R* = 0.054 (*wR* = 0.066) for 1655 independent reflections; (3), C₂₆H₂₀O₂·2C₆H₇N, *M_r*

= 550.67, triclinic, *P* $\bar{1}$, *a* = 8.371 (5), *b* = 9.599 (2), *c* = 10.182 (2) Å, α = 71.12 (1), β = 82.05 (3), γ = 74.45 (3)°, *V* = 744.6 (5) Å³, *Z* = 1, *D_m* = 1.226 (3), *D_x* = 1.228 Mg m⁻³, Mo *K*α, λ = 0.7107 Å, μ = 0.070 mm⁻¹, *F*(000) = 292, *T* = 294 K, final *R* = 0.041 (*wR* = 0.040) for 1932 independent reflections; (4), C₂₆H₂₀O₂·C₆H₇N, *M_r* = 457.57, triclinic, *P* $\bar{1}$, *a* = 9.337 (2), *b* = 10.407 (3), *c* = 13.470 (9) Å, α = 70.75 (3), β = 87.65 (3), γ = 73.58 (2)°, *V* = 1183.2 (9) Å³, *Z* = 2, *D_m* = 1.271 (4), *D_x* = 1.284 Mg m⁻³, Mo *K*α, λ = 0.7107 Å, μ = 0.074 mm⁻¹, *F*(000) = 484, *T* = 294 K, final *R* = 0.060 (*wR* = 0.065) for 2530 independent reflections. For compounds (2)–(4), a qualitative inverse correlation between the O···N hydrogen-bond distances and ΔH of the guest-release reaction is observed.

Introduction

The ability of the host *trans*-9,10-dihydroxy-9,10-diphenyl-9,10-dihydroanthracene (*H*) to form inclusion compounds with a variety of guest molecules (Toda, 1987; Tanaka, Toda & Mak, 1984; Toda,

Tanaka & Mak, 1984, 1985; Toda, Tanaka, Nagamatsu & Mak, 1985) has prompted us to undertake a study of selected complexes with the aim of establishing the types and strengths of their host-guest interactions.



Studies of this kind can provide information which is useful for the rational design of host molecules whose selectivity towards particular structural and optical isomers finds application in industrial separation processes (Toda, 1987). Previous X-ray and thermoanalytical studies of inclusion compounds of the title host have been confined to alcohol and ketone guests. The complex with an ethanol guest (Toda *et al.*, 1984) is characterized by host-host O—H...O hydrogen bonding, with ethanol molecules attaching laterally to infinite chains of host molecules *via* acceptor hydrogen bonds whereas in crystals of the complexes containing methanol (Toda, Tanaka, Nagamatsu & Mak, 1985) and 1,4-butanediol (Toda, Tanaka & Mak, 1985) pairs of guest molecules serve as double bridges between host molecules forming hydrogen-bonded (OH)₄ rings. The structures and thermal behaviour of the complexes with acetophenone, 3-methylcyclopentanone (Bond, Nassimbeni & Toda, 1989*a*), and the isomers 2- and 4-methylcyclohexanone (Bond, Nassimbeni & Toda, 1989*b*) have been described. In these species the host:guest ratio is 1:2 and the structures are characterized by O—H...O=C hydrogen bonds which link host and guest. Centrosymmetry of the host molecule requires both —OH functions to be engaged in these bonds so that the repeating motif in the crystal is invariably a 1:2 molecular complex. Heating each complex leads to loss of its guest in a single step; this is followed by melting of the host between 526 and 551 K.

We have recently isolated a 1:1 complex of the same host with a 2-butanone guest. This unexpected stoichiometry prompted structural investigation and comparison with the above findings. This study was extended to include inclusion compounds of the title host with substituted pyridine guests, for which no detailed investigations have yet appeared in the literature. Crystals of a 1:2 complex with 4-vinylpyridine as well as crystals containing the isomers 2- and 4-methylpyridine (stoichiometries 1:1 and 1:2 respectively) were isolated and their characterization by X-ray analysis, thermal gravimetric analysis (TGA) and differential scanning calorimetry (DSC) is reported here.

Experimental

The host compound was prepared as previously described (Bond *et al.*, 1989*a*). Suitable crystals of the molecular complexes were obtained by slow evaporation from dilute solutions of the host in the appropriate guest. The time required ranged from two days [compound (1)] to seven days [compound (4)]. Preliminary characterization included density determination (flotation in aqueous KI), microanalysis using a Heraeus universal combustion analyser, Model CHN-Rapid, melting-point determination on a Linkam TH600 hot stage coupled to a Linkam C0600 temperature controller and thermal analysis. DSC measurements were performed using a Du Pont 9900 differential scanning calorimeter calibrated with indium and zinc. Sample masses were in the range 6–126 mg and the heating rate was 10 K min⁻¹ over the interval 293–623 K. For TGA measurements, a Du Pont 9900 thermogravimetric analyser calibrated with CuSO₄·5H₂O as standard was employed. Sample masses ranged from 6 to 14 mg and the heating rate was 10 K min⁻¹ under a constant positive N₂ flow. X-ray powder patterns for the four compounds and their products after guest desorption were recorded on a Philips PW1050/80 diffractometer using Cu K α radiation ($\lambda = 1.5418 \text{ \AA}$) with divergence and receiving slits 1° each. Samples were scanned at 1° 2 θ min⁻¹ over the range $8 \leq 2\theta \leq 40^\circ$. Preliminary cell dimensions and space-group data were obtained from Weissenberg and precession photographs (Cu K α radiation). Satisfactory intensity data collections were obtained with crystals of (1) and (4) mounted in Lindemann capillaries [(1) in the presence of a saturated solution of the complex] and (2) and (3) mounted on glass fibres.

Intensity data collection

Enraf-Nonius CAD-4 diffractometer, graphite-monochromated Mo K α radiation; ω -2 θ scans, final acceptance limit 20σ at 20° min⁻¹ in ω , maximum recording time 40 s and $(\sin\theta/\lambda)_{\max} = 0.595 \text{ \AA}^{-1}$. Intensities of three standard reflections checked every hour and orientation control every 200 measured reflections. Data corrected for Lp effects and for absorption using in each case azimuthal scans for nine reflections with χ near 90°; absorption corrections from the program EAC (Enraf-Nonius package).

Structure solution

Structures solved by direct methods using SHELX76 (Sheldrick, 1976) for compounds (1)–(3) and SHELXS86 (Sheldrick, 1985) for (4). Centrosymmetry confirmed by intensity statistics. Location and refinement of atoms of host generally followed

Table 1. *Crystal data, experimental and refinement parameters*

	(1)	(2)	(3)	(4)
Molecular formula	C ₂₆ H ₂₀ O ₂ ·C ₆ H ₆ O	C ₂₆ H ₂₀ O ₂ ·2C ₆ H ₇ N	C ₂₆ H ₂₀ O ₂ ·2C ₆ H ₇ N	C ₂₆ H ₂₀ O ₂ ·C ₆ H ₇ N
Molecular weight (g mol ⁻¹)	436.55	574.72	550.67	457.57
Space group	P $\bar{1}$	P2 ₁ /c	P $\bar{1}$	P $\bar{1}$
a (Å)	7.924 (1)	10.045 (2)	8.371 (5)	9.337 (2)
b (Å)	8.827 (2)	18.630 (3)	9.599 (2)	10.407 (3)
c (Å)	9.050 (1)	8.419 (4)	10.182 (2)	13.470 (9)
α (°)	109.93 (2)	90	71.12 (1)	70.75 (3)
β (°)	97.31 (1)	96.29 (3)	82.05 (3)	87.65 (3)
γ (°)	97.65 (1)	90	74.45 (3)	73.58 (2)
Z	1	2	1	2
V (Å ³)	579.5 (2)	1566.0 (9)	744.6 (5)	1183.2 (9)
D _x (g cm ⁻³)	1.251	1.219	1.228	1.284
D _m (g cm ⁻³) (floatation in aqueous KI)	1.248 (4)	1.208 (3)	1.226 (3)	1.271 (4)
μ (Mo K α) (cm ⁻¹)	0.74	0.70	0.70	0.74
F(000)	232	608	292	484
Data collection (294 K)				
Crystal dimensions (mm)	0.38 × 0.50 × 0.50	0.22 × 0.25 × 0.41	0.16 × 0.19 × 0.50	0.34 × 0.38 × 0.38
Range scanned θ (°)	1 ≤ θ ≤ 25	1 ≤ θ ≤ 25	1 ≤ θ ≤ 25	1 ≤ θ ≤ 25
Range of indices	-9 ≤ h ≤ 9, -10 ≤ k ≤ 10, 0 ≤ l ≤ 10	-11 ≤ h ≤ 11, 0 ≤ k ≤ 22, 0 ≤ l ≤ 10	-9 ≤ h ≤ 9, -11 ≤ k ≤ 11, 0 ≤ l ≤ 12	-11 ≤ h ≤ 11, -12 ≤ k ≤ 12, 0 ≤ l ≤ 16
No. of reflections for lattice parameters, θ range (°)	24, 16 ≤ θ ≤ 17	24, 16 ≤ θ ≤ 17	24, 16 ≤ θ ≤ 17	24, 16 ≤ θ ≤ 17
Indices of standard reflections	512, 243, 116	752, 4.11.3, 236	228, 474, 564	482, 369, 631
Intensity variation for standard reflections (%)	+2.3	+0.3	+1.5	-10.5
Scan width (°)	0.85 + 0.35tan θ	0.90 + 0.35tan θ	0.90 + 0.35tan θ	0.85 + 0.35tan θ
Vertical aperture length (mm)	4	4	4	4
Aperture width (mm)	1.12 + 1.05tan θ	1.12 + 1.05tan θ	1.12 + 1.05tan θ	1.20 + 1.45tan θ
Max. scan time (s)	40	40	40	40
No. of reflections collected	2183	3047	2764	5665
No. of unique reflections	1885	2292	2322	3536
R _{int}	0.012	0.017	0.012	0.023
No. of reflections observed with I _{rel} > 2 σ (I _{rel})	1690	1655	1932	2530
Final refinement				
No. of parameters	165	214	201	330
R	0.059	0.054	0.041	0.060
wR	0.077	0.066	0.040	0.065
w	$[\sigma^2(F_o) + 0.02609F_o^2]^{-1}$	$[\sigma^2(F_o) + 6.647 \times 10^{-3}F_o^2]^{-1}$	$[\sigma^2(F_o)]^{-1}$	$[\sigma^2(F_o) + 1.554 \times 10^{-3}F_o^2]^{-1}$
S	0.689	0.759	2.525	1.994
Max. shift/e.s.d.	1.5	0.11	1.9	0.17
Average shift/e.s.d.	0.038	0.022	0.07	0.001
Max. height in difference Fourier map (e Å ⁻³)	0.28	0.23	0.15	0.28
Min. height in difference Fourier map (e Å ⁻³)	-0.33	-0.23	-0.16	-0.26
Absorption corrections, min., max., average	0.9849, 0.9999, 0.9922	0.9884, 0.9997, 0.9947	0.9873, 0.9986, 0.9979	0.8680, 0.9896, 0.8955

by difference Fourier syntheses which revealed guest atoms. In (1) and (4), guests disordered in two alternative orientations (discussed below). H atoms located in difference Fourier syntheses and (except for the hydroxylic host H atom) placed in idealized positions (C—H 1.08 Å) with common varying U_{iso} values for chemically similar groups. Full-matrix least-squares refinement on F (SHELX76) minimizing $\sum w||F_o| - |F_c||^2$ with all non-H atoms thermally anisotropic. Complex neutral-atom scattering factors for non-H atoms from Cromer & Mann (1968), for H atoms from Stewart, Davidson & Simpson (1965); dispersion corrections from Cromer & Liberman (1970). Molecular parameters from PARST (Nardelli, 1983) and illustrations drawn with PLUTO89 (Motherwell, 1989) from the PC version of NRCVAX. Crystal data and details of data collections and refinements are given in Table 1.

Results and discussion

Fractional atomic coordinates for complexes (1)–(4) are given in Table 2, and bond lengths and angles in Tables 3 and 4 respectively. Hydrogen-bond data are

listed in Table 5.* The compound *trans*-9,10-dihydroxy-9,10-diphenyl-9,10-dihydroanthracene is hereafter referred to as the host.

Host structure

The host molecules in compounds (1)–(4) occupy centrosymmetric sites. Endocyclic torsion angles in the central 1,4-cyclohexadiene ring are all less than 3° yielding asymmetry parameters ΔC_s and ΔC_2 (Duax & Norton, 1975) less than 0.3°. This low value indicates an essentially planar central moiety, as previously reported for this host (Bond *et al.*, 1989*a,b*). As the maximum out-of-plane deviation of any C atom from the fused phenyl rings is only 0.006 (2) Å, the entire tricyclic system is effectively planar in all cases. Dihedral angles between the planes of the tricyclic system and the phenyl substituents are in the range 84.3 (1) to 89.1 (1)°.

* Lists of structure factors, anisotropic thermal parameters, H-atom parameters and torsion angles have been deposited with the British Library Document Supply Centre as Supplementary Publication No. SUP 53265 (64 pp.). Copies may be obtained through The Technical Editor, International Union of Crystallography, 5 Abbey Square, Chester CH1 2HU, England.

Table 2. Fractional atomic coordinates ($\times 10^4$) and thermal parameters ($\text{\AA}^2 \times 10^3$) with *e.s.d.*'s in parentheses

$U_{eq} = \frac{1}{3}(\text{trace of the orthogonalized } U_i \text{ matrix}).$

Compound (1)	x	y	z	U_{iso}^*/U_{eq}
C(1)	-64 (2)	1567 (2)	1382 (2)	34 (1)
O(1)	1307 (2)	2973 (2)	2185 (2)	48 (1)
H(1)	2306 (47)	2879 (46)	1949 (47)	108 (12)*
C(2)	509 (2)	73 (2)	1620 (2)	34 (1)
C(3)	1005 (2)	164 (3)	3193 (2)	43 (1)
C(4)	1504 (3)	-1150 (3)	3511 (2)	52 (1)
C(5)	1491 (3)	-2587 (3)	2255 (3)	54 (1)
C(6)	1035 (3)	-2689 (2)	697 (2)	46 (1)
C(7)	536 (2)	-1362 (2)	363 (2)	35 (1)
C(11)	-1627 (2)	1912 (2)	2187 (2)	34 (1)
C(12)	-3116 (2)	712 (2)	1712 (2)	44 (1)
C(13)	-4537 (3)	967 (3)	2442 (3)	53 (1)
C(14)	-4491 (3)	2442 (3)	3659 (3)	56 (1)
C(15)	-3025 (3)	3646 (3)	4136 (2)	57 (1)
C(16)	-1600 (3)	3402 (2)	3396 (2)	46 (1)
C(50)	-4326 (4)	-4243 (5)	250 (6)	102 (2)
O(50)†	-3778 (6)	-3810 (6)	-625 (6)	100 (2)
C(60)	-3624 (6)	-3375 (5)	2056 (5)	110 (2)

Compound (2)	x	y	z	U_{iso}^*/U_{eq}
C(1)	5030 (3)	778 (1)	5583 (3)	42 (1)
O(1)	4624 (2)	1412 (1)	4700 (3)	53 (1)
H(1)	4155 (41)	1279 (21)	3854 (49)	73 (12)*
C(2)	3823 (3)	285 (2)	5658 (3)	39 (1)
C(3)	2706 (3)	567 (2)	6258 (4)	52 (1)
C(4)	1584 (3)	150 (2)	6395 (4)	60 (1)
C(5)	1584 (3)	-561 (2)	5899 (4)	59 (1)
C(6)	2676 (3)	-842 (2)	5296 (4)	50 (1)
C(7)	3820 (3)	-423 (1)	5151 (3)	40 (1)
C(11)	5543 (3)	1020 (1)	7277 (3)	39 (1)
C(12)	5620 (3)	1736 (2)	7701 (4)	48 (1)
C(13)	6102 (4)	1936 (2)	9241 (4)	62 (1)
C(14)	6497 (4)	1430 (2)	10377 (4)	62 (1)
C(15)	6419 (3)	715 (2)	9970 (4)	62 (1)
C(16)	5940 (3)	508 (2)	8445 (4)	51 (1)
N(21)	2726 (3)	1257 (2)	1962 (4)	68 (1)
C(22)	1579 (4)	900 (2)	1789 (5)	69 (1)
C(23)	577 (3)	1020 (2)	593 (4)	63 (1)
C(24)	706 (3)	1544 (2)	-495 (4)	56 (1)
C(25)	1905 (4)	1921 (2)	-376 (4)	70 (1)
C(26)	2883 (4)	1760 (2)	885 (5)	75 (2)
C(27)	-409 (4)	1694 (2)	-1768 (5)	78 (1)
C(28)	-486 (6)	2219 (3)	-2714 (7)	123 (3)

Compound (3)	x	y	z	U_{iso}^*/U_{eq}
C(1)	-66 (2)	-1659 (2)	390 (2)	40 (1)
O(1)	1249 (2)	-2921 (2)	242 (2)	53 (1)
H(1)	2136 (35)	-2524 (32)	-478 (32)	143 (12)*
C(2)	428 (2)	-971 (2)	1377 (2)	39 (1)
C(3)	851 (2)	-1929 (2)	2712 (2)	50 (1)
C(4)	1280 (3)	-1388 (3)	3678 (2)	58 (1)
C(5)	1303 (3)	127 (3)	3331 (2)	58 (1)
C(6)	903 (2)	1076 (2)	2026 (2)	51 (1)
C(7)	466 (2)	541 (2)	1031 (2)	39 (1)
C(11)	-1588 (2)	-2299 (2)	1049 (2)	41 (1)
C(12)	-1505 (3)	-3835 (2)	1485 (2)	53 (1)
C(13)	-2906 (3)	-4364 (3)	2125 (2)	67 (1)
C(14)	-4378 (3)	-3362 (3)	2298 (2)	67 (1)
C(15)	-4476 (3)	-1830 (3)	1839 (2)	62 (1)
C(16)	-3088 (2)	-1293 (2)	1222 (2)	50 (1)
N(21)	3858 (2)	7769 (2)	8271 (2)	58 (1)
C(22)	5279 (3)	6775 (3)	8680 (2)	58 (1)
C(23)	6563 (3)	6350 (2)	7783 (2)	55 (1)
C(24)	6409 (3)	6984 (2)	6373 (2)	52 (1)
C(25)	4939 (3)	8027 (2)	5941 (2)	59 (1)
C(26)	3726 (3)	8373 (3)	6905 (3)	62 (1)
C(27)	7785 (3)	6542 (3)	5345 (3)	87 (1)

Compound (4)	x	y	z	U_{iso}^*/U_{eq}
C(1)	566 (3)	6192 (3)	9257 (2)	38 (1)
O(1)	731 (2)	6463 (2)	8144 (2)	47 (1)
H(1)	483 (42)	5704 (43)	7920 (31)	86 (13)*
C(2)	-1076 (3)	6359 (3)	9474 (2)	35 (1)
C(3)	-2110 (3)	7668 (3)	8962 (3)	45 (1)
C(4)	-3617 (3)	7878 (4)	9106 (3)	53 (2)
C(5)	-4129 (3)	6788 (3)	9763 (3)	51 (2)
C(6)	-3119 (3)	5495 (3)	10269 (3)	45 (1)
C(7)	-1587 (3)	5259 (3)	10139 (2)	37 (1)

Table 2 (cont.)

	x	y	z	U_{iso}^*/U_{eq}
C(11)	1074 (3)	7336 (3)	9516 (2)	38 (1)
C(12)	1152 (4)	7289 (4)	10554 (3)	48 (2)
C(13)	1659 (4)	8268 (4)	10802 (3)	58 (2)
C(14)	2095 (4)	9317 (4)	10032 (4)	61 (2)
C(15)	2007 (4)	9377 (3)	9001 (3)	60 (2)
C(16)	1490 (3)	8395 (3)	8743 (3)	48 (1)
C(1B)	671 (3)	4558 (3)	6127 (2)	36 (1)
O(1B)	-72 (2)	4795 (2)	7034 (2)	43 (1)
H(1B)	-1029 (57)	5350 (52)	6857 (40)	125 (19)*
C(2B)	-19 (3)	3638 (3)	5737 (2)	36 (1)
C(3B)	-43 (3)	2319 (3)	6454 (3)	48 (1)
C(4B)	-607 (4)	1399 (3)	6161 (3)	54 (2)
C(5B)	-1164 (4)	1784 (4)	5136 (3)	52 (2)
C(6B)	-1173 (3)	3085 (3)	4424 (3)	45 (1)
C(7B)	-601 (3)	4025 (3)	4711 (2)	35 (1)
C(11B)	2299 (3)	3732 (3)	6500 (2)	38 (1)
C(12B)	3359 (3)	3652 (4)	5745 (3)	57 (2)
C(13B)	4829 (4)	2856 (5)	6050 (4)	73 (2)
C(14B)	5258 (4)	2135 (4)	7109 (4)	70 (2)
C(15B)	4220 (4)	2233 (4)	7853 (3)	60 (2)
C(16B)	2745 (3)	3031 (3)	7555 (3)	45 (1)
N(21)‡	2909 (7)	3157 (8)	3374 (5)	48 (2)*
C(22)‡	4193 (7)	3400 (7)	3073 (5)	54 (2)*
C(23)‡	5511 (12)	2195 (10)	3179 (7)	67 (2)*
C(24)‡	5268 (10)	907 (12)	3569 (7)	75 (3)*
C(25)‡	3965 (10)	681 (9)	3846 (7)	85 (3)*
C(26)‡	2772 (11)	1832 (10)	3754 (7)	73 (3)*
C(27)‡	4260 (13)	4866 (12)	2645 (9)	96 (4)*
N(31)‡	-2927 (7)	-3694 (9)	-3191 (5)	44 (2)*
C(32)‡	-3547 (9)	-2254 (9)	-3514 (6)	47 (2)*
C(33)‡	-5104 (11)	-1662 (14)	-3441 (8)	59 (3)*
C(34)‡	-5912 (12)	-2643 (11)	-3054 (8)	66 (3)*
C(35)‡	-5373 (10)	-3958 (10)	-2809 (7)	68 (3)*
C(36)‡	-3882 (11)	-4510 (12)	-2843 (8)	65 (3)*
C(37)‡	-2470 (12)	-1395 (12)	-3916 (9)	73 (4)*

† S.o.f. = 0.5.
‡ S.o.f. = 0.45.
§ S.o.f. = 0.55.

Table 3. Bond lengths (\AA) with *e.s.d.*'s in parentheses

	(1)	(2)	(3)	(4)	(4B)
C(1)—O(1)	1.440 (2)	1.433 (3)	1.434 (2)	1.440 (4)	1.438 (4)
C(1)—C(2)	1.523 (3)	1.528 (4)	1.521 (3)	1.521 (4)	1.522 (5)
C(1)—C(11)	1.528 (2)	1.529 (4)	1.538 (3)	1.540 (5)	1.530 (4)
O(1)—H(1)	0.85 (4)	0.87 (4)	1.03 (3)	1.02 (5)	0.91 (5)
C(2)—C(3)	1.400 (3)	1.384 (5)	1.402 (3)	1.398 (3)	1.400 (4)
C(2)—C(7)	1.389 (2)	1.386 (4)	1.386 (3)	1.392 (4)	1.392 (4)
C(3)—C(4)	1.380 (4)	1.384 (5)	1.376 (4)	1.377 (4)	1.379 (6)
C(4)—C(5)	1.383 (3)	1.389 (5)	1.386 (4)	1.382 (5)	1.383 (6)
C(5)—C(6)	1.378 (3)	1.364 (5)	1.373 (3)	1.377 (4)	1.375 (5)
C(6)—C(7)	1.398 (3)	1.407 (4)	1.401 (3)	1.395 (4)	1.398 (5)
C(11)—C(12)	1.388 (2)	1.381 (4)	1.381 (3)	1.387 (5)	1.396 (4)
C(11)—C(16)	1.390 (2)	1.397 (4)	1.393 (2)	1.379 (4)	1.385 (4)
C(12)—C(13)	1.382 (3)	1.384 (5)	1.397 (4)	1.373 (7)	1.385 (4)
C(13)—C(14)	1.382 (3)	1.369 (5)	1.374 (3)	1.380 (6)	1.389 (7)
C(14)—C(15)	1.377 (3)	1.377 (5)	1.374 (4)	1.374 (7)	1.373 (6)
C(15)—C(16)	1.389 (3)	1.376 (5)	1.386 (3)	1.388 (6)	1.388 (4)
C(1)—C(7)	1.518 (3)	1.520 (4)	1.515 (2)	1.513 (3)	1.519 (4)
C(50)—O(50)	1.101 (8)				
C(50)—C(60)	1.539 (6)				
C(50)—C(50 ⁱⁱ)	1.489 (5)				
N(21)—C(22)		1.324 (5)	1.331 (3)	1.315 (10)	
N(21)—C(26)		1.326 (5)	1.330 (3)	1.345 (13)	
C(22)—C(23)		1.362 (5)	1.375 (3)	1.460 (11)	
C(22)—C(27)				1.461 (14)	
C(23)—C(24)		1.355 (5)	1.375 (3)	1.350 (16)	
C(24)—C(25)		1.388 (5)	1.384 (3)	1.320 (14)	
C(24)—C(27)		1.489 (5)	1.514 (4)		
C(25)—C(26)		1.398 (5)	1.364 (4)	1.360 (12)	
C(27)—C(28)		1.259 (7)			
N(31)—C(32)				1.368 (12)	
N(31)—C(36)				1.367 (15)	
C(32)—C(33)				1.423 (13)	
C(32)—C(37)				1.499 (16)	
C(33)—C(34)				1.391 (18)	
C(34)—C(35)				1.250 (14)	
C(35)—C(36)				1.353 (13)	

Symmetry codes: compound (1), (i) $-x, -y, -z$; (ii) $-1-x, -1-y, -z$; compound (2), (i) $1-x, -y, 1-z$; compound (3), (i) $-x, -y, -z$; compound (4), (i) $-x, 1-y, 2-z$; compound (4B), (i) $-x, 1-y, 1-z$.

Table 4. Bond angles ($^{\circ}$) with *e.s.d.*'s in parentheses

	(1)	(2)	(3)	(4)	(4B)
C(2)—C(1)—C(11)	108.7 (2)	109.1 (2)	108.6 (2)	109.8 (4)	108.3 (4)
O(1)—C(1)—C(11)	107.1 (2)	106.8 (2)	106.7 (2)	105.8 (3)	106.4 (3)
O(1)—C(1)—C(2)	108.8 (2)	109.6 (2)	109.2 (2)	108.7 (3)	109.6 (4)
C(1)—O(1)—H(1)	117 (3)	107 (3)	109 (2)	111 (2)	111 (3)
C(1)—C(2)—C(7)	123.3 (2)	122.3 (3)	123.6 (2)	122.8 (4)	123.8 (4)
C(1)—C(2)—C(3)	117.5 (2)	117.7 (3)	117.5 (2)	118.1 (4)	117.6 (4)
C(3)—C(2)—C(7)	119.2 (2)	120.0 (3)	119.0 (2)	119.1 (4)	118.6 (4)
C(2)—C(3)—C(4)	121.1 (2)	121.2 (4)	121.1 (2)	121.0 (4)	121.5 (5)
C(3)—C(4)—C(5)	119.4 (2)	118.9 (3)	119.7 (2)	120.1 (4)	119.5 (5)
C(4)—C(5)—C(6)	120.3 (2)	120.4 (4)	119.8 (3)	119.3 (4)	119.9 (5)
C(5)—C(6)—C(7)	120.7 (2)	121.1 (3)	121.1 (2)	121.6 (4)	121.1 (5)
C(2)—C(7)—C(6)	119.3 (2)	118.4 (3)	119.3 (2)	118.9 (4)	119.3 (4)
C(1)—C(11)—C(16)	121.7 (2)	119.7 (3)	118.7 (2)	121.7 (4)	122.3 (4)
C(1)—C(11)—C(12)	119.6 (2)	121.9 (3)	122.0 (2)	119.6 (4)	118.6 (4)
C(12)—C(11)—C(16)	118.7 (2)	118.3 (3)	119.3 (2)	118.8 (4)	119.1 (4)
C(11)—C(12)—C(13)	121.1 (2)	120.4 (4)	119.9 (2)	120.2 (5)	120.2 (5)
C(12)—C(13)—C(14)	119.9 (2)	121.0 (4)	120.4 (3)	121.1 (5)	120.2 (5)
C(13)—C(14)—C(15)	119.6 (2)	119.2 (4)	119.9 (3)	118.9 (5)	119.6 (5)
C(14)—C(15)—C(16)	120.8 (2)	120.5 (4)	120.2 (3)	120.3 (5)	120.6 (5)
C(11)—C(16)—C(15)	119.9 (2)	120.6 (4)	120.2 (3)	120.6 (5)	120.3 (5)
O(1)—C(1)—C(7)	109.4 (2)	109.5 (2)	109.5 (2)	109.3 (3)	109.6 (3)
C(11)—C(1)—C(7)	109.2 (1)	108.3 (3)	109.3 (2)	109.3 (3)	109.9 (3)
C(2)—C(1)—C(7)	113.5 (2)	113.4 (2)	113.4 (2)	113.7 (3)	112.8 (3)
C(6)—C(7)—C(1)	117.6 (2)	117.3 (2)	117.7 (2)	117.6 (3)	117.3 (3)
C(2)—C(7)—C(1)	123.2 (2)	124.3 (3)	123.1 (2)	123.5 (3)	123.4 (3)
O(50)—C(50)—C(60)	121.0 (5)				
C(50 ^a)—C(50)—C(60)	116.8 (5)				
C(50 ^a)—C(50)—O(50)	122.0 (5)				
C(22)—N(21)—C(26)		116.6 (4)	116.1 (3)	121.8 (8)	
N(21)—C(22)—C(23)		124.2 (4)	123.9 (2)	119.0 (8)	
N(21)—C(22)—C(27)				119.1 (8)	
C(23)—C(22)—C(27)				121.9 (9)	
C(22)—C(23)—C(24)		120.1 (3)	119.4 (3)	115.1 (10)	
C(23)—C(24)—C(27)		120.1 (3)	121.3 (2)		
C(23)—C(24)—C(25)		117.5 (4)	117.0 (2)	125.3 (12)	
C(25)—C(24)—C(27)		122.3 (3)	121.8 (2)		
C(24)—C(25)—C(26)		118.6 (4)	119.7 (2)	117.7 (10)	
N(21)—C(26)—C(25)		123.0 (4)	124.0 (3)	121.1 (10)	
C(24)—C(27)—C(28)		126.2 (5)			
C(32)—N(31)—C(36)				116.7 (9)	
N(31)—C(32)—C(37)				115.2 (9)	
N(31)—C(32)—C(33)				120.6 (9)	
C(33)—C(32)—C(37)				124.3 (10)	
C(32)—C(33)—C(34)				115.3 (11)	
C(33)—C(34)—C(35)				124.7 (12)	
C(34)—C(35)—C(36)				119.3 (11)	
N(31)—C(36)—C(35)				123.2 (11)	

Symmetry codes: compound (1), (i) $-x, -y, -z$; (ii) $-1-x, -1-y, -z$; compound (2), (i) $1-x, -y, 1-z$; compound (3), (i) $-x, -y, -z$; compound (4), (i) $-x, 1-y, 2-z$; compound (4B), (i) $-x, 1-y, 1-z$.

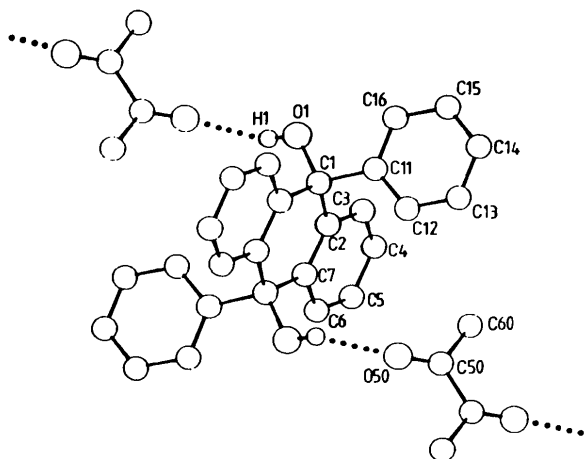


Fig. 1. Perspective view of compound (1). The guest 2-butanone is disordered on a $\bar{1}$ site [s.o.f. of O(50) is 0.5]. For clarity only one H atom is included. Dotted lines indicate hydrogen bonds.

Crystal structures

Atomic numbering for (1) is shown in Fig. 1. To satisfy space-group requirements, one formula unit $C_{26}H_{26}O_2 \cdot C_4H_8O$ of (1) can be accommodated in the unit cell with the host located at a centre of symmetry and the unsymmetrical 2-butanone molecule disordered over two related general sites or at a second symmetry centre. A difference Fourier map phased with the centre of the host molecule at 0,0,0 revealed three peaks near $\frac{1}{2}, \frac{1}{2}, 0$, one of which was within

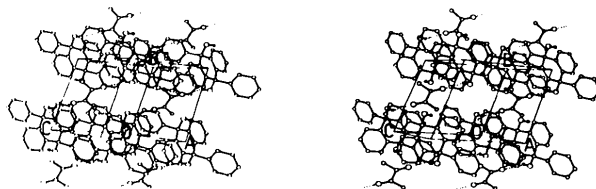


Fig. 2. Stereoview of the molecular packing in (1). Hydrogen bonds are indicated by dotted lines.

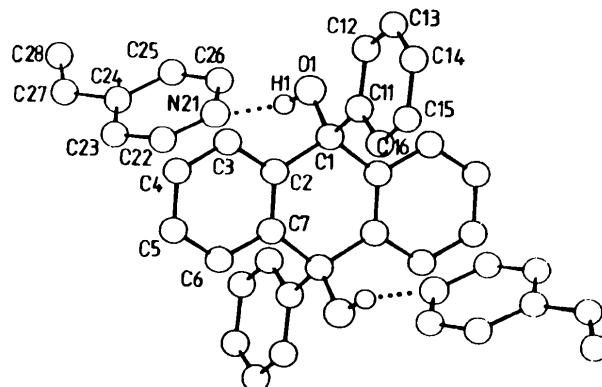


Fig. 3. Perspective view of compound (2). For clarity only one H atom is included. Dotted lines represent hydrogen bonds.

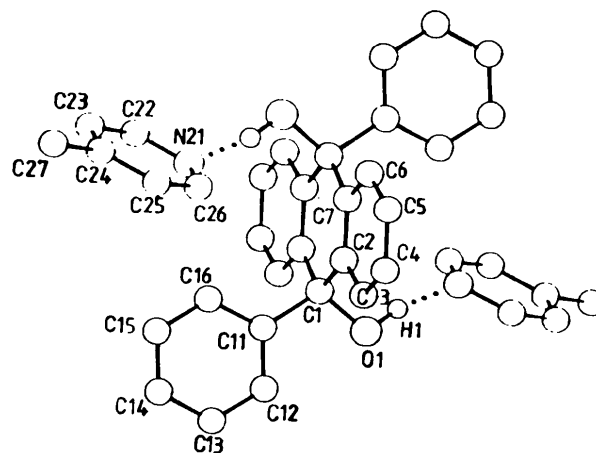


Fig. 4. Perspective view of compound (3). For clarity only one H atom is included. Dotted lines represent hydrogen bonds.

Table 5. *Hydrogen-bond distances (Å) and angles (°) for compounds (1)–(4)*

Compound (1)					
O(1)···O(50 ⁱ)	2.721 (6)	H(1)···O(50 ⁱ)	2.06 (5)	O(1)—H(1)···O(50 ⁱ)	134 (4)
Compound (2)					
O(1)···N(21)	2.841 (4)	H(1)···N(21)	2.00 (4)	O(1)—H(1)···N(21)	163 (4)
Compound (3)					
O(1)···N(21 ⁱⁱ)	2.817 (3)	H(1)···N(21 ⁱⁱ)	1.81 (3)	O(1)—H(1)···N(21 ⁱⁱ)	168 (3)
Compound (4)					
O(1)···O(1B)	2.892 (4)	H(1)···O(1B)	1.91 (5)	O(1)—H(1)···O(1B)	160 (4)
O(1B)···N(21 ⁱⁱⁱ)	2.831 (6)	H(1B)···N(21 ⁱⁱⁱ)	1.94 (5)	O(1B)—H(1B)···N(21 ⁱⁱⁱ)	166 (5)
O(1B)···N(31 ^{iv})	2.656 (6)	H(1B)···N(31 ^{iv})	1.76 (5)	O(1B)—H(1B)···N(31 ^{iv})	167 (5)

Symmetry codes: (i) $-x, -y, -z$; (ii) $x, -1 + y, -1 + z$; (iii) $-x, 1 - y, 1 - z$; (iv) $x, 1 + y, 1 + z$.

bonding distance of its centrosymmetric counterpart. The planar array of six peaks was interpreted as the superposition of two 2-butanone molecules related by $\bar{1}$, the carbonyl O atom having a site-occupancy factor (s.o.f.) of 0.5. Inclusion in the refinement of atoms C(50) and C(60) each with a unit s.o.f. and O(50) with an s.o.f. of 0.5 led to a very significant reduction in R from 0.245 (host alone) to 0.094 (host plus guest) and a reasonable molecular geometry for the guest, thus vindicating this model for guest disorder. Guest H atoms were included with appro-

appropriate s.o.f.'s. The molecular packing (Fig. 2) reveals that the guest molecules occupy channels parallel to [001], each guest carbonyl O atom being hydrogen-bonded to the host —OH function (Table 5).

Recent structural studies of molecular inclusion complexes of the same host with the ketones, acetophenone, 3-methylcyclopentanone, 2- and 4-methylcyclohexanone (Bond *et al.*, 1989*a,b*) have shown

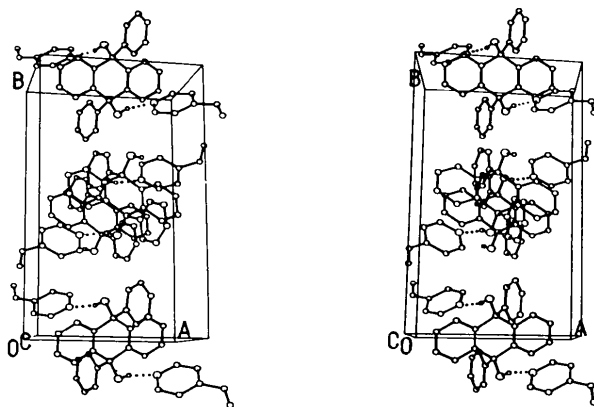


Fig. 5. Stereoview showing the molecular packing in (2). Hydrogen bonds are indicated by dotted lines.

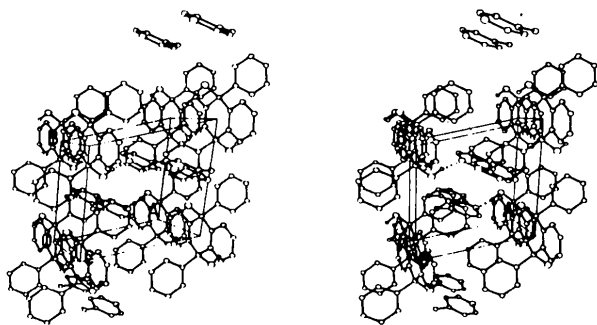


Fig. 6. Stereoview showing the molecular packing in (3). Hydrogen bonds are indicated by dotted lines.

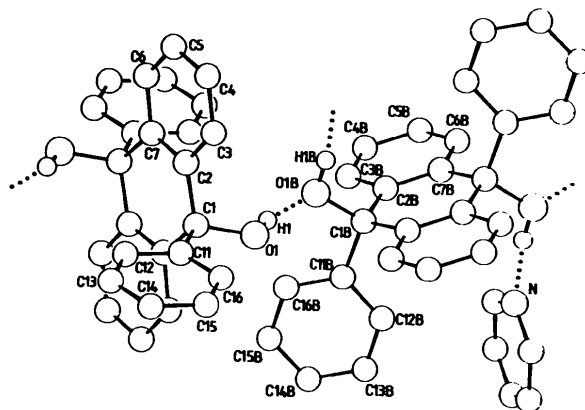


Fig. 7. Perspective view of complex (4). For clarity, only two H atoms are included and the pyridine ring represents the average ring position for the disordered 2-methylpyridine guest molecule. Hydrogen bonds are indicated by dotted lines.

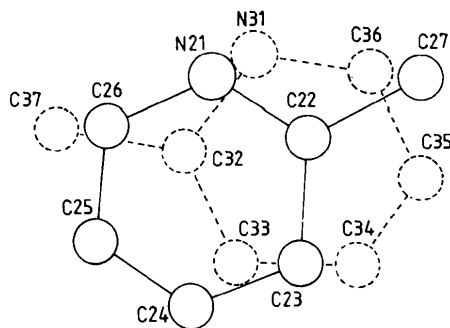


Fig. 8. Two alternative orientations found for the guest 2-methylpyridine in complex (4). The molecule containing atom N(21) has an s.o.f. of 0.55. (Reported coordinates for the two molecules are related through the inversion centre at 0,0,0.)

that a 1:2 host:guest ratio is the norm, with the host molecule located at a centre of symmetry and hydrogen-bonded ($-\text{OH}\cdots\text{O}=\text{C}$) to two ketone molecules.

Complexes (2) and (3) share structural similarities as a result of a common 1:2 host:guest ratio and the space-group constraints which require the host molecule to be located at a centre of symmetry while the guest molecules, 4-vinylpyridine and 4-methylpyridine respectively, occupy general positions (Figs. 3 and 4). Each host molecule is thus associated with two guest molecules *via* $\text{O}-\text{H}\cdots\text{N}$ hydrogen bonds

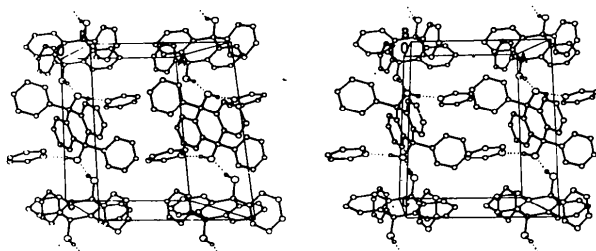


Fig. 9. Stereoview showing molecular packing in complex (4). The aromatic ring of the guest 2-methylpyridine is shown in its average position. Hydrogen bonds are indicated by dotted lines.

(Table 5). In this respect, (2) and (3) are structural analogues of the 1:2 ketone complexes discussed previously. The $\text{O}-\text{H}\cdots\text{N}$ hydrogen bonds and general van der Waals contacts are the only sources of cohesion in crystals of (2) and (3) as there is no evidence of parallel stacking of the substituted pyridine molecules either with themselves or with host phenyl rings. Figs. 5 and 6 show the molecular packing arrangements in (2) and (3) respectively.

On replacing the guest 4-methylpyridine in (3) by its isomer 2-methylpyridine in (4), an unexpected change in host:guest ratio from 1:2 to 1:1 without a change in space group occurred. The large unit-cell volume of (4) does, however, require $Z = 2$, and the two crystallographically independent host molecules were found to occupy Wyckoff positions (*c*) and (*g*) in $P\bar{1}$ with the guest 2-methylpyridine in a general position. Atomic numbering is shown in Fig. 7. Owing to guest disorder, Fig. 7 includes for simplicity only the aromatic ring of the guest in the average position derived from the two alternative positions found. The latter are coplanar and are related by an approximate mirror plane perpendicular to their mean plane, the separation $\text{N}(21)\cdots\text{N}(31)$ being only $0.54(1) \text{ \AA}$ (Fig. 8). The 'average' guest ring position

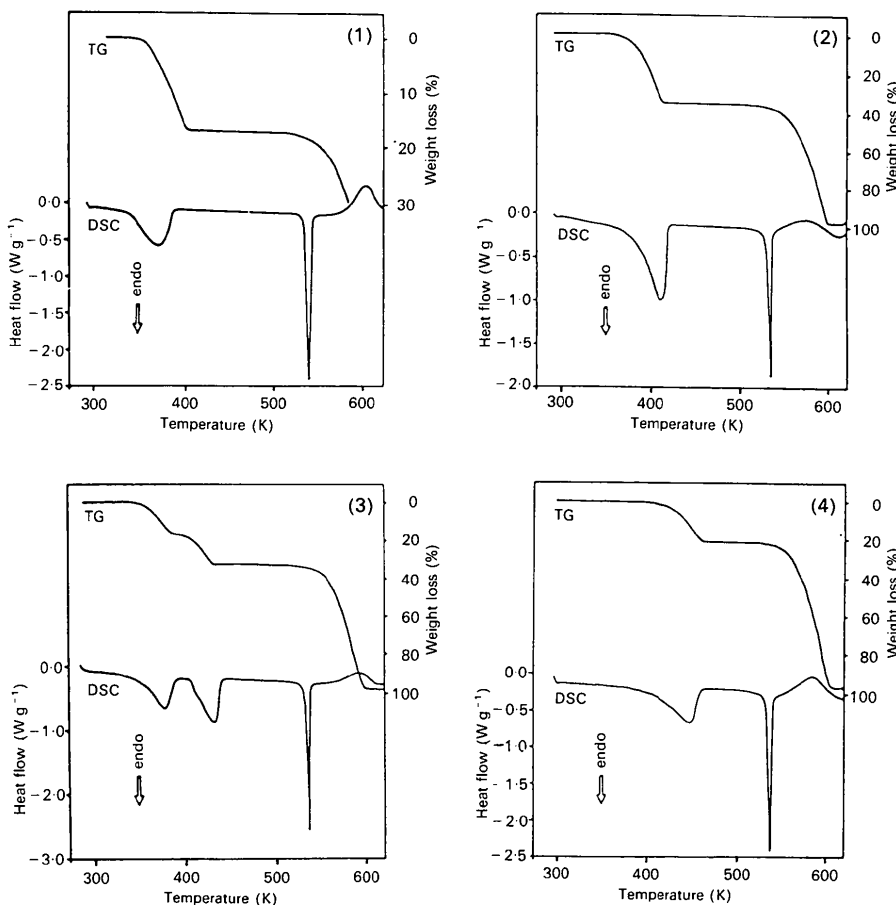


Fig. 10. TG and DSC traces for compounds (1)–(4).

Table 6. *Thermal analyses results*

Reaction*	Calc. weight loss (%)	Measured weight loss (%)	Onset temp. (K)	ΔH (J g ⁻¹)	ΔH (kJ mol ⁻¹)	O—H...N O—H...O (Å)
Compound (1) $H_2C_6H_8O \rightarrow H + C_6H_8O$	16.5	16.5	342	78.1	34.1	2.721 (6)
Compound (2) $H_2C_6H_7N \rightarrow H + 2C_6H_7N$	36.6	36.1	383	132.6	72.2	2.841 (4)
Compound (3) $H_2C_6H_7N \rightarrow H + C_6H_7N + C_6H_7N$	16.9	16.2	355	61.3	33.8	2.817 (3)
$H_2C_6H_7N \rightarrow H + C_6H_7N$	33.8	32.5	408	82.6	45.5	
Compound (4) $H_2C_6H_7N \rightarrow H + C_6H_7N$	20.4	21.5	410	91.9	42.1	2.831 (6) 2.656 (6)

* $H = C_{26}H_{20}O_2$.

depicted in Figs. 7 and 9 was obtained by averaging pairs of atomic coordinates (excluding those of the methyl substituents) so as to yield a ring orientation intermediate between those shown in Fig. 8. The existence of the two alternative orientations shown (s.o.f.'s 0.55 and 0.45) implies that the ordered host framework in complex (4) provides cavities which could accommodate molecules somewhat larger than 2-methylpyridine. Of the four structures described here, that of (4) is unique in containing, in addition to host-guest (O—H...N) hydrogen bonds, host-host O—H...O hydrogen bonds (Table 5). The latter give rise to infinite chains of host molecules directly linked along the *z* direction, every alternate host molecule being hydrogen bonded to two guest molecules (Fig. 9).

The host-guest ratios of the four compounds were confirmed by TGA and the enthalpy of the guest-release reactions was determined by DSC. The thermograms are shown in Fig. 10, and for each compound the percentage weight loss (Table 6) is in excellent agreement with the theoretical value, never differing by more than 2%.

For compounds (1), (2) and (4), the TG curves show that the loss of guest molecules is a single-step process, which is accompanied by a corresponding endotherm. This is followed by a sharp endotherm at 535 K which corresponds to the melting point of the host compound. In compound (3), however, the guest molecules are released in two distinct steps, the first starting at 355 K and corresponding to the loss of one guest molecule, while the release of the second guest begins at 408 K.

The formation of an inclusion compound, followed by its decomposition with host and guest upon heating, can follow two fundamentally different paths. This is illustrated in Fig. 11 which depicts the host molecules in their unclathrated, α phase. When dissolved directly in the liquid guest, a new β or clathrate phase is formed. The mechanism of this process is not fully understood, but the guest molecule, because of its shape and the resulting host-

guest interactions, probably acts as a template for the new structure.

When the inclusion compound is heated and the guest molecules are allowed to escape, the host may revert to its former α phase, or the host framework may hold, giving rise to an 'empty' clathrate, or β_0 phase. A well known example of the latter phenomenon is in zeolites, which can be dehydrated by heating to elevated temperatures under vacuum without significant damage to the silica/alumina framework (Barrer, 1978). We have investigated this phenomenon by X-ray powder diffraction. Compounds (1), (2) and (4) were analysed at room temperature. Each was then heated under vacuum until the guest loss was complete. This was checked gravimetrically in each case. The resulting powder was again analysed by X-ray diffraction, and in each case the diffraction pattern corresponded to the unclathrated α phase (Toda, Tanaka, Nagamatsu & Mak, 1985). Compound (3), however, has a two-step desorption process and therefore it was heated under

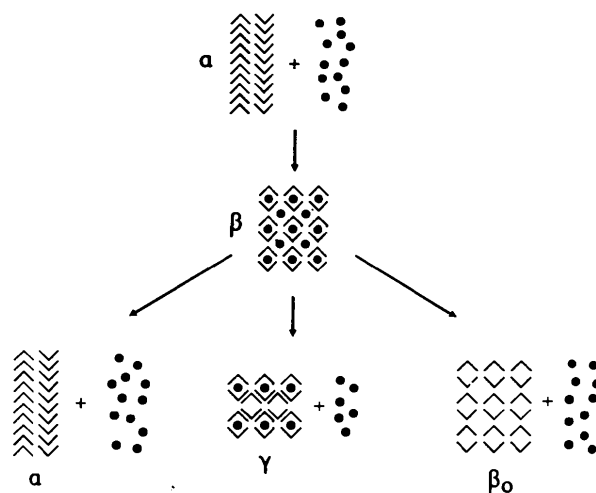


Fig. 11. Schematic diagram showing possible decomposition paths of inclusion compounds.

vacuum to 403 K. At this point the percentage weight loss corresponded to the loss of one guest molecule and the X-ray powder pattern was distinctly different from that of either the starting compound or the final pattern corresponding to the α phase of the host. We have therefore identified a new compound of host:guest stoichiometry 1:1, which corresponds to the γ phase shown in Fig. 11. The X-ray diffraction patterns for compound (3) are shown in Fig. 12.

The object of carrying out thermal analysis on these compounds is to reconcile thermodynamics

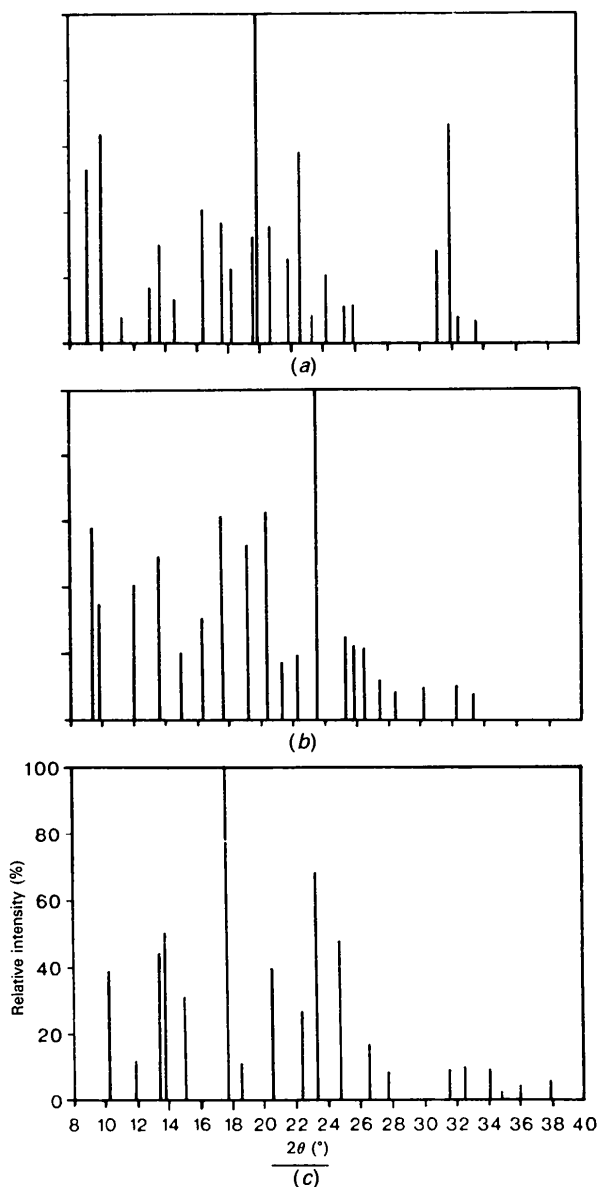


Fig. 12. Powder diffraction patterns for compound (3): (a) before heating, (b) after heating to 403 K (loss of one guest molecule), (c) after complete guest loss (identical to pattern for host alone).

with structure. Thus it should, in principle, be possible to find a relationship between the measured enthalpies of the guest-release reactions and the structures of the clathrates. This problem has been discussed for a number of clathrate systems such as the Werner clathrates (Moore, Nassimbeni & Niven, 1987), which entrap a variety of organic guest molecules, and the Hofmann clathrates (Sopková & Šingliar, 1984) which have been used for chromatographic separation of guest mixtures. A similar aspect of this structure-activity comparison is correlation of the threshold temperature of desolvation of water molecules in various hydrates with crystal packing and hydrogen bonding (Byrn, 1982).

In the present study one might expect correlation between the O...N hydrogen-bond distance and ΔH of the guest-release reaction for compounds (2), (3) and (4), and the data are detailed in Table 6. Various difficulties arise, however. Compound (2) releases both guests in a single step with a ΔH of 72.2 kJ mol⁻¹ or 36.1 kJ per mole of guest, while in compound (3) the two guests are released singly and with differing enthalpy change values of 33.8 and 45.5 kJ mol⁻¹, averaging 39.7 kJ mol⁻¹. In compound (4) the guest molecules are disordered and the O...N distances vary considerably, averaging 2.744 (6) Å, with a ΔH of 42.1 kJ mol⁻¹. There is therefore at least a qualitative inverse correlation between O...N hydrogen-bond length and the ΔH of the guest-release reaction, but further work will have to be carried out in order to confirm this trend. We are therefore extending the study of these inclusion compounds to encompass a variety of other substituted pyridines.

We thank the University of Cape Town and the Foundation for Research Development (Pretoria) for research grants.

References

- BARRER, R. M. (1978). *Zeolites and Clay Minerals as Sorbents and Molecular Sieves*. London: Academic Press.
- BOND, D. R., NASSIMBENI, L. R. & TODA, F. (1989a). *J. Inclusion Phenom. Mol. Recognition Chem.* **7**, 623-635.
- BOND, D. R., NASSIMBENI, L. R. & TODA, F. (1989b). *J. Crystallogr. Spectrosc. Res.* **19**, 847-859.
- BYRN, S. R. (1982). *Solid State Chemistry of Drugs*, ch. 5. London: Academic Press.
- CROMER, D. T. & LIBERMAN, D. (1970). *J. Chem. Phys.* **53**, 1891-1898.
- CROMER, D. T. & MANN, J. B. (1968). *Acta Cryst.* **A24**, 321-325.
- DUAX, W. L. & NORTON, D. A. (1975). Editors. *Atlas of Steroid Structure*, Vol. 1. London: Plenum Press.
- MOORE, M. H., NASSIMBENI, L. R. & NIVEN, M. L. (1987). *Inorg. Chim. Acta*, **131**, 45-52.
- MOTHERWELL, W. D. S. (1989) *PLUTO89*. Program for plotting molecular and crystal structures. Univ. of Cambridge, England.
- NARDELLI, M. (1983). *Comput. Chem.* **7**, 95-98.

- SHELDRIK, G. M. (1976). *SHELX76*. Program for crystal structure determination. Univ. of Cambridge, England.
- SHELDRIK, G. M. (1985). *SHELXS86*. *Crystallographic Computing 3*, edited by G. M. SHELDRIK, C. KRÜGER & R. GODDARD, pp. 175–189. Oxford Univ. Press.
- SOPKOVÁ, A. & ŠINGLIAR, M. (1984). *Inclusion Compounds*, Vol. 3, ch. 7, pp. 245–256. London: Academic Press.
- STEWART, R. F., DAVIDSON, E. R. & SIMPSON, W. T. (1965). *J. Chem Phys.* **42**, 3175–3187.
- TANAKA, K., TODA, F. & MAK, T. C. W. (1984). *J. Inclusion Phenom.* **2**, 99–102.
- TODA, F. (1987). *Top. Curr. Chem.* **140**, 43–69.
- TODA, F., TANAKA, K. & MAK, T. C. W. (1984). *Tetrahedron Lett.* **25**, 1359–1362.
- TODA, F., TANAKA, K. & MAK, T. C. W. (1985). *J. Inclusion Phenom.* **3**, 225–233.
- TODA, F., TANAKA, K., NAGAMATSU, S. & MAK, T. C. W. (1985). *Isr. J. Chem.* **25**, 346–352.

Acta Cryst. (1990). **B46**, 780–784

Redetermination of the Structure of Methyl *p*-Dimethylaminobenzenesulfonate at Two Temperatures

BY JAGARLAPUDI A. R. P. SARMA* AND JACK D. DUNITZ

Organic Chemistry Laboratory, Swiss Federal Institute of Technology, ETH-Zentrum, CH-8092 Zürich, Switzerland

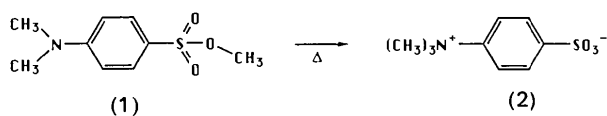
(Received 16 January 1990; accepted 13 June 1990)

Abstract

$C_9H_{13}NO_3S$, $M_r = 215.29$, monoclinic, $P2_1/c$; $a = 8.855$ (2), $b = 10.426$ (5), $c = 11.082$ (3) Å, $\beta = 91.13$ (2)°, $V = 1022.9$ (5) Å³ at 193 K; $a = 8.913$ (1), $b = 10.487$ (4), $c = 11.166$ (2) Å, $\beta = 90.95$ (1)°, $V = 1043.5$ (4) Å³ at 255 K; $Z = 4$, $D_x = 1.40$ g cm⁻³ at 193 K (1.37 g cm⁻³ at 255 K), Mo $K\alpha$ radiation, $\lambda = 0.7107$ Å, $\mu = 2.84$ (2.78) cm⁻¹, $F(000) = 456$, $R = 0.054$ (0.044) for 963 (876) observed reflections with $I \geq 3\sigma(I)$. The crystal structure of methyl *p*-dimethylaminobenzenesulfonate has been redetermined at 193 and 255 K. Motional analysis and packing potential-energy calculations support the view [Sukenic, Bonapace, Mandel, Lau, Wood & Bergman (1977). *J. Am. Chem. Soc.* **99**, 851–858] that the thermally induced methyl transfer reaction which takes place in this crystal is assisted by cooperative motions of the molecules in stacks running along the **b** direction.

Introduction

One of the most interesting thermal solid-state reactions is the conversion (see scheme below) of methyl *p*-dimethylaminobenzenesulfonate (1) to the zwitter-



* Present address: Indian Institute of Chemical Technology, Hyderabad, 500 007 India.

ionic product *p*-trimethylammonobenzenesulfonate (2) (Kuhn & Ruelius, 1950). Later Sukenic, Bonapace, Mandel, Lau, Wood & Bergman (1977) showed that the reaction is intermolecular and proceeds much faster in the crystal than it does either in the melt or in solution. They determined the crystal structure of (1), which contains stacks of molecules nearly ideally oriented for the intermolecular methyl transfer. From EHT (extended Hückel theory) calculations, Gavezzotti & Simonetta (1977) proposed a two-step mechanism, involving a molecular ion-pair intermediate, but they did not discuss the possibility of correlated motions of molecules within the stacks. Menger, Kaiserman & Scotchie (1984) showed that the reaction proceeds faster in the bulk crystal than on the surface, where an unidentified reaction intermediate accumulates; however, no such intermediate was detectable in the bulk. From Raman phonon spectroscopic measurements, Dwarakanath & Prasad (1980) suggested that softening of a lattice vibration mode (27 cm⁻¹ at 163 K) plays an important role in the reaction. In support of this, Prasad (1987) made a motional analysis of the crystal structure results of Sukenic *et al.* (1977) and found the major rigid-body motion to be libration about the long molecular axis. Since the accuracy of the room-temperature crystal structure suffers from several factors [use of Cu radiation; slow crystal decomposition (~22% in three days); intensity standards reduced by 60%], we thought it worthwhile to make new structure analyses at lower temperatures. We report these results here, together with results of packing-energy calculations.